

Effect of mobilised length on the performance of a paddled energy-absorbing rockbolt

DL Venter *Epiroc, Australia*

G Knox *Epiroc, South Africa*

Abstract

Energy-absorbing rockbolts have become widely accepted as a best practice where the anticipated failure mode of the rock mass may result in rockbursts. The prolific application of the paddled energy-absorbing rockbolt within the industry is a result of the installation method and the energy capacity demonstrated through laboratory impact testing and a series of well-documented field trials. The design of the paddled energy-absorbing rockbolt is a debonding length of smooth steel bounded by two anchor points. When a load is applied to the rockbolt, the debonding length of steel bar is mobilised and plastically deforms, absorbing energy. Consequently, the capacity of the rockbolt is directly correlated to the mechanical and geometric properties of the steel bar from which it is produced. The specific capacity of a paddled energy-absorbing rockbolt is determined through split tube impact testing, and it is common practice to calculate an energy absorption rate in kJ/m. Due to the limited data and geometric constraints of the test equipment, these values are often used to calculate the capacity of a rockbolt when the length of the debonding length varies. The variation in the debonded length can result from either a relocation of the anchor points along the length of the rockbolt or a variation in the length of the rockbolt.

This paper presents the results of a controlled investigation demonstrating the effect of the debonding length on the performance of a paddled energy-absorbing rockbolt through a series of laboratory-based impact tests. The debonding length of the paddled energy-absorbing rockbolt was varied by altering the length of the tendons produced from the same batch of steel, to limit the variation in the mechanical properties of the samples. The investigation demonstrates that the practice of extrapolating to longer mobilised lengths, using data generated from shorter debonded length samples, can result in an over estimation of the energy absorption capacity of a rockbolt.

Keywords: *rock reinforcement design, dynamic impact testing, debonded length, energy-absorbing rockbolt*

1 Introduction

As mines go deeper, the risk of stress-induced and seismic damage to underground excavations increases. To protect excavations, ground support design and application are becoming increasingly critical to ensure the safety and productivity of mining operations (Kaiser & Moss 2022). When the field stress in the rock wall of an excavation in brittle rock is high relative to the in situ strength of the rock mass, large displacements may occur due to the gradual bulking of the stress-fractured rock (Kaiser & Moss 2022). In addition, large displacements may occur due to sudden violent bulking of the rock wall during rockbursts, induced by dynamic loading (Kaiser & Moss 2022). Rockbolts reinforcing the rock wall in which large displacements are expected are required not only to have sufficient load capacity, but also to provide sufficient deformation capacity (Kaiser & Moss 2022). The rockbolts should therefore be able to absorb a large amount of energy prior to rupture (Li 2010).

The paddled energy-absorbing rockbolt has been widely adopted within the mining industry for applications in challenging ground conditions where significant deformation of the rock wall is expected. The bolt is fully grouted within a borehole by resin or cement. It consists of paddled anchor points, which are firmly fixed in the grout. Between the anchor points is a smooth section of bar with a very weak bond with the grout (Li 2010). When the rock mass dilates between the paddled anchor points, the entire smooth section of the

bar debonds from the grout and is mobilised (Li & Doucet 2012). The debonded length of bar yields after a small amount of deformation and deforms plastically until its maximum strain limit is reached (Li 2010).

Various laboratory test campaigns have been undertaken to better understand the behaviour of paddled energy-absorbing rockbolts under various loading conditions (Li 2010; Li & Doucet 2012; Bosman et al. 2018; Knox et al. 2018a, 2018b; Knox & Berghorst 2018a, 2018b). The test samples used during these campaigns generally had a specific configuration and length. The ‘mobilised’ or ‘debonded’ length of the test samples was frequently limited by the maximum rockbolt length that a specific dynamic test rig could accommodate. Due to this limitation, the energy absorption capacity of rockbolts with longer debonded lengths is frequently extrapolated from the average dynamic test results of a sample set of rockbolts with a shorter debonded length. The basic assumption is that there is a linear relationship between the energy absorption capacity and the debonded length of the rockbolt. Although this assumption seems logical, it has not been adequately tested and verified. In addition, using an average kJ/m value calculated from a specific sample set does not necessarily account for the variability of the energy absorption capacity of the specific material.

Li & Doucet (2012) compared the energy absorption capacity for a sample set of Ø22 mm D-Bolt rockbolts with a 900 and 1,500 mm debonded length, respectively, and observed a linear relationship between the energy absorption capacity and debonded length. However, the input energies used during the dynamic impact tests were different for the respective debonded length sample sets. Bosman et al. (2018) observed that higher input energy during a dynamic impact test result in a lower total energy absorption capacity of a rockbolt.

This paper describes the methodology and the results of an investigation into the effect of the mobilised length on the dynamic performance of the PAR1 Resin Bolt during dynamic impact testing. The investigation was conducted under laboratory-controlled conditions and resulted in consistent and repeatable results.

2 Paddled energy-absorbing rockbolt

A paddled energy-absorbing rockbolt, illustrated in Figure 1, is designed for application in rockmasses where the anticipated failure mode of the host rock will result in rockbursting. The rockbolt is comprised of a base element, which is a smooth steel bar onto which paddle sets and a thread is formed by plastically deforming the steel (Li 2010). The paddle sets perform the function of mixing the resin medium during installation and once the resin has cured, anchoring the bar within the medium. During loading of the rockbolt, the smooth bar debonds from the resin and elongates. Li (2010) stated that the bar debonds from the chemical medium along the entire mobilised length of the bar. Therefore, it can be assumed that the interface between the smooth bar and resin has a zero-magnitude cohesion and adhesion during loading. Consequently, the performance of the rockbolt is defined by the mechanical properties of the steel and dimensional properties of the bar. The length of each element of the rockbolt is defined by the configuration; typically, the variations of the length of the rockbolt result in changes to the ‘debonded’ length of the bar.

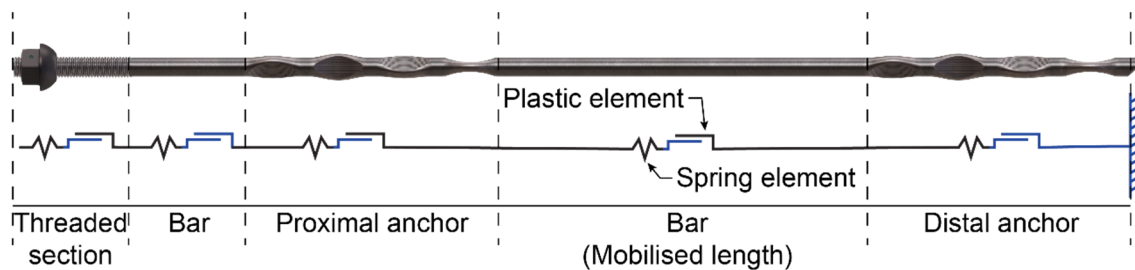


Figure 1 Illustration representing the components of the PAR1 Resin Bolt

Considering the paddled energy-absorbing rockbolt illustrated in Figure 1 and assuming the position of the proximal anchor relative to the threaded end of the bolt is constant, the length of the debonded section correlates to the total length of the rockbolt. Considering the displacement potential of the rockbolt, each

element of the rockbolt can thus be represented by a combination of a spring element (elastic strain) and a plastic element (plastic strain), as represented in Figure 1.

2.1 Phases of steel strain

The elongation properties of the rockbolt are defined by the strain properties of the steel bar from which the rockbolt is produced. Steel is defined as a homogeneous material. During loading, the material deforms through four phases: elastic strain, Lüders strain, plastic strain, and ultimately necking strain. To understand the effect of the change in debonding length of padded energy-absorbing rockbolt, the strain phases illustrated in Figure 2 are reviewed. During the initial loading, below the yield stress, the strain is defined as elastic strain, no permanent deformation of the material occurs during this phase, and the strain is defined as uniform across the entire mobilised length of the sample. Once the yield stress (σ_y) of the material is exceeded, permanent deformation of the steel commences during plastic strain, which is uniform across the entire loaded length of the material. The uniform deformation of the steel is maintained until the stress in the material rises to the point that the ultimate stress (σ_u) of the material is achieved. At this point the strain in the material is localised to the portion of the sample which is necking prior to rupture. As the necking strain is localised, the deformation which occurs during necking is relatively consistent for a given material and independent of the loaded length of the sample.

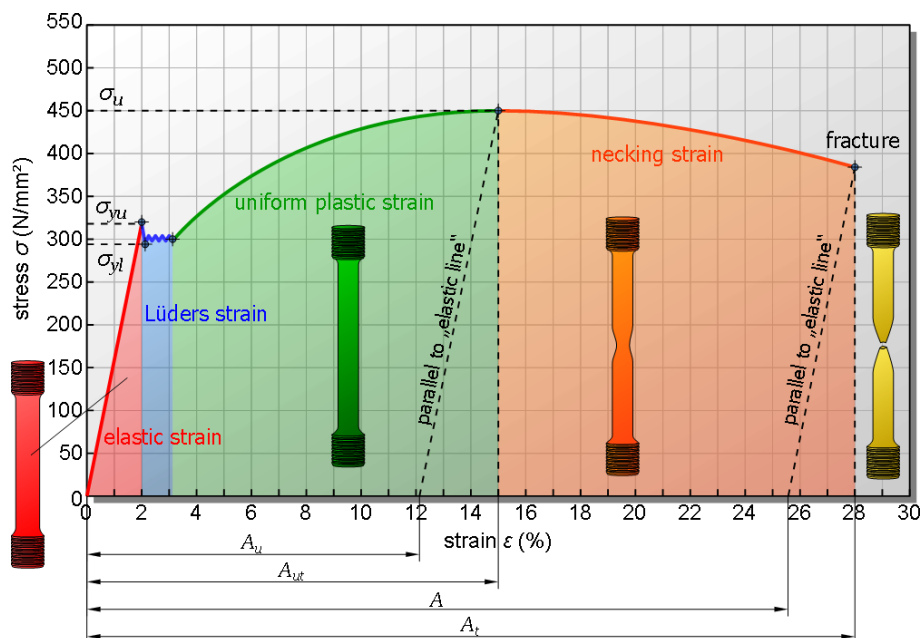


Figure 2 Strain phases of steel during loading (Tech Science 2018)

The elongation that occurs during the necking strain phase is localised and independent of the length of the sample (constant). The plastic strain (A_u) can be considered as uniform or global strain and is directly dependent on the length of sample. The total strain can be represented as per Equation 1. Elongation of the necking is independent of the length of the sample, hence, the contribution of the necking strain to the strain at fracture (A_t) is dependent on the length of the samples. Consequently, material testing standards (International Organisation for Standardisation 2019; ASTM International 2022) define a standard gauge length (L_0), defined by Equation 2, over which the strain properties of a material are determined. S_0 is defined as the cross-sectional area of the sample.

$$\epsilon \approx \frac{(\epsilon_{elastic} + \epsilon_{plastic}) \times Length + \delta_{necking}}{Length} \quad (1)$$

$$L_0 = k \times \sqrt{S_0} \quad (2)$$

To illustrate the effect of sample length on the total strain of a sample during quasi-static loading, samples ranging in length from 100 to 3,000 mm in increments of 500 mm were pulled axially to destruction. The test aimed to illustrate the plastic deformation capacity of the material from which the PAR1 Resin Bolt is manufactured. Figure 3 illustrates the increase in deformation capacity with an increase in the mobilised length of steel. This is a logical and expected observation. However, the data also illustrates the phenomenon of dilution of the necking strain contribution to the total strain of the sample. At shorter lengths, the necking strain contributes significantly to the strain at rupture. However, as the deformation that occurs during the necking strain phase is relatively consistent, the contribution to strain at rupture is diluted as the length of the sample increases. Thus, the strain at rupture tends toward the uniform component of the strain, which is dependent on the length of the sample and, therefore, the strain at ultimate stress (A_u).

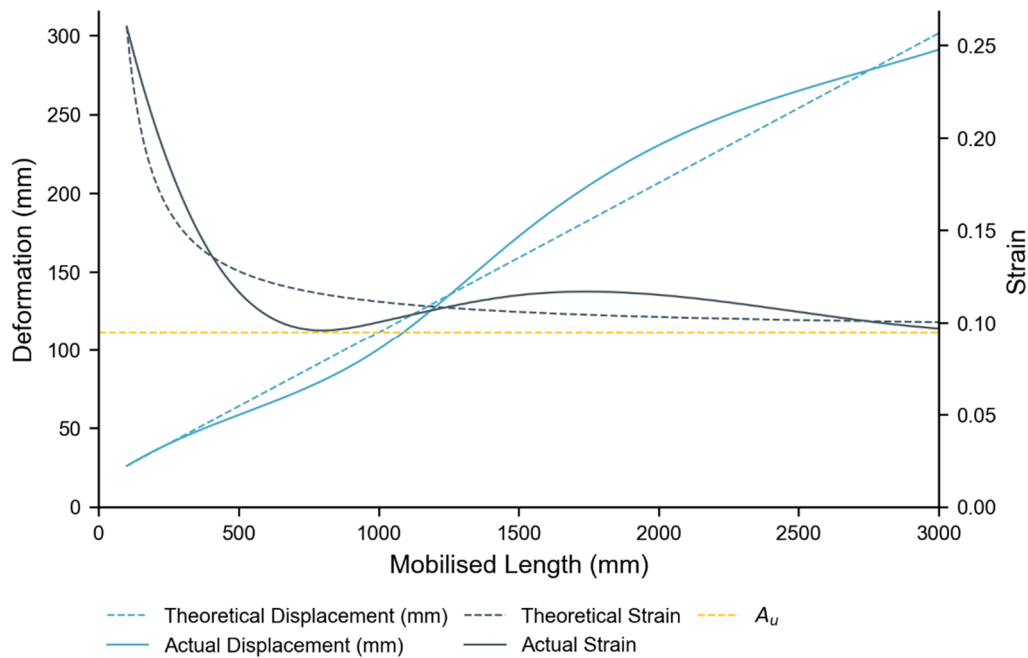


Figure 3 Theoretical versus actual displacement and strain against the mobilised length of steel

2.2 PAR1 Resin Bolt

The PAR1 Resin Bolt, illustrated in Figure 4, is a padded energy-absorbing rockbolt designed and manufactured by Epiroc (2023). It has two padded sets (Figure 4a) of four paddles (Figure 4c) phased at 45° between consecutive paddles (Figure 4b). The paddle configuration was developed to optimise the mixing of the capsule resin and anchorage within the cured resin matrix. The position of the proximal paddle set may be varied; however, it is typically located at 450 mm from the proximal end (threaded end) of the bolt to which the nut is affixed.

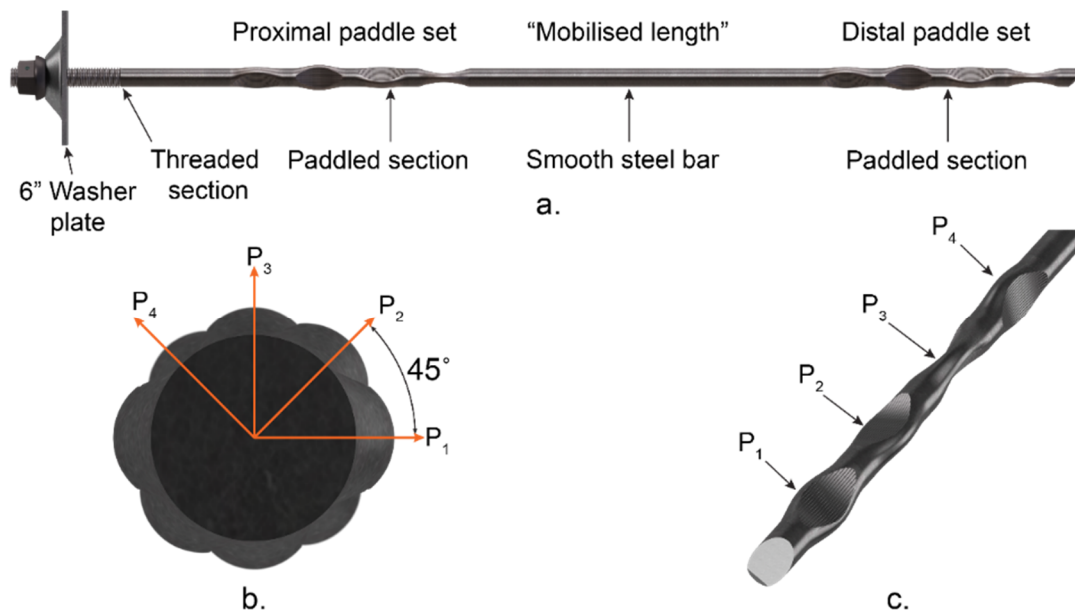


Figure 4 Layout of a PAR1 Resin Bolt (Knox & Hadjigeorgiou 2022)

3 Dynamic impact testing of PAR1 Resin Bolt

Dynamic impact testing is a common method used to test energy-absorbing rockbolts. The limitations of this method are well known; however, it provides an efficient and repeatable method to test various rockbolt types and designs for comparison under controlled conditions (Hadjigeorgiou & Potvin 2011). The debonded length of test samples is frequently limited by the maximum rockbolt length that a specific test rig can accommodate. Due to this limitation, the energy absorption capacity of rockbolts with longer debonded lengths is frequently extrapolated from the average dynamic test results of a sample set of rockbolts with a shorter debonded length. The average total energy absorbed for a specific sample set is divided by the debonded length to calculate an average kJ/m value. To calculate the energy absorption capacity for a longer debonded length, the kJ/m value is multiplied by the full debonded length.

The purpose of the investigation was to determine the effect of varying the ‘debonded’ or ‘mobilised’ length between the paddles of an energy-absorbing rockbolt on the capacity of the rockbolt, determined through impact testing. The impact tests were conducted on the PAR1 Resin Bolt. For practical purposes, the ‘debonded’ length was altered by reconfiguring the distal paddle set position (Figure 5). The position of the paddle set relative to the proximal end of the bolt was fixed at 450 mm, and the length of the rockbolt was changed to adjust the ‘debonded’ length of the paddled energy-absorbing rockbolt.

3.1 Sample preparation

Three sample batches with different lengths of the $\varnothing 20$ mm PAR1 Resin Bolt were prepared and installed for this investigation. The samples referenced and the length of the ‘debonding’ section of the rockbolt are defined in Figure 5. The rockbolts were all produced from the same cast of steel. This was to mitigate the effect of variations in steel on the comparison between the free lengths. The typical installation process for a PAR1 Resin Bolt with two speed resin cartridges is illustrated in Figure 6.

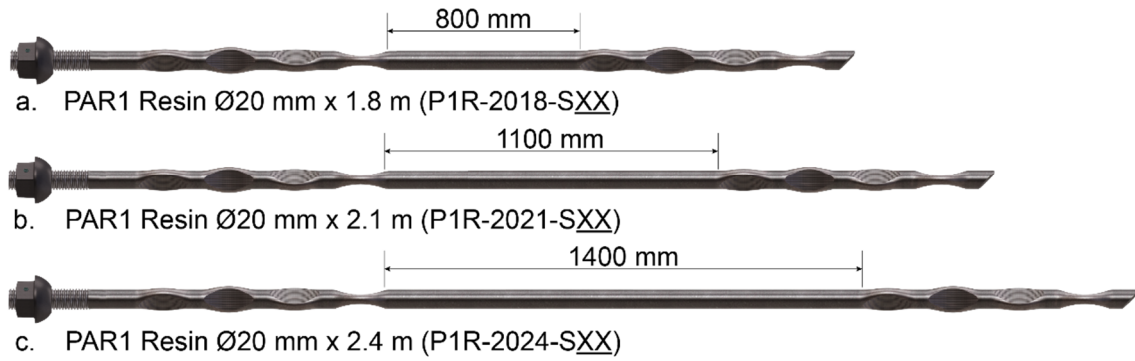


Figure 5 Illustration of the mobilised steel length for the three PAR1 Resin Bolt samples

As the rate of rotation, rate of insertion and spin time all affect the quality of the resin mixture, the installations were completed on an installation rig where the parameters of the installation could be controlled to ensure consistency between the samples. A single 60-second resin capsule was placed in the distal end of the host tube, and the remainder of the resin capsules installed were a 5-minute set resin.

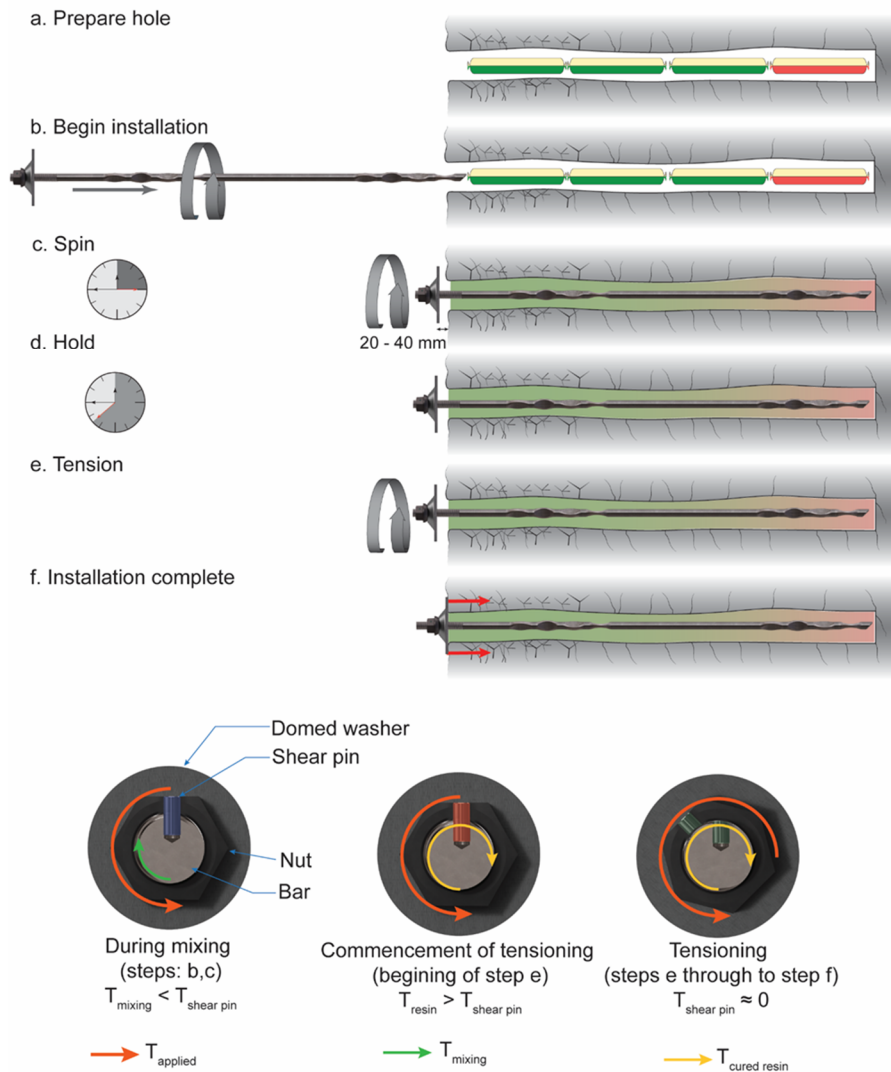


Figure 6 Installation process for a paddled energy-absorbing rockbolt in resin (Knox & Hadjigeorgiou 2022)

The length of the host tube, consisting of a hollow bar with a $\varnothing 56$ mm outside diameter and a $\varnothing 35$ mm internal diameter, was configured to be 160 mm shorter than the length of the rockbolt. The location of the split was placed at the approximate midpoint between the proximal and distal anchor sets, as illustrated in Figure 7b. After installation, the installed samples were cured for at least an hour prior to instrumentation for impact testing. All samples were prepared and instrumented for an indirect impact split tube testing. The configuration of the instrumentation is illustrated in Figure 7a.

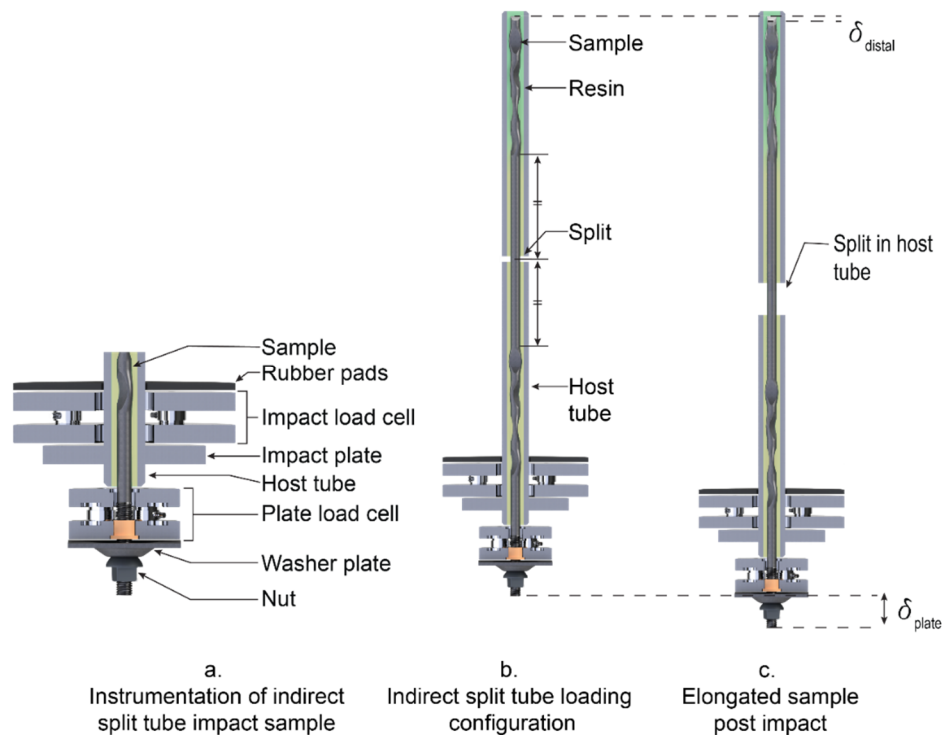


Figure 7 Sample instrumentation: (a) Instrumentation of the load cells; (b) Location of the split in the host tube; (c) Representation of the displacement metrics recorded (Knox & Hadjigeorgiou 2022)

3.2 Dynamic impact tester

The impact tests were conducted using the Epiroc dynamic impact tester (DIT) in Figure 8. The DIT has been designed in accordance with ASTM D7401-08 (ASTM International 2008). The machine is designed to impart an impulse of energy into a rockbolt, installed in a host tube, by raising a known mass to a known height and then releasing the mass to impact the sample. The specifications of the machine are shown in Table 1. The construction of the machine and details of the instrumentation have been documented by Knox & Berghorst (2018a) and Knox & Hadjigeorgiou (2022). During an impact, the load and displacement of the rockbolt are recorded and processed to determine the total displacement and calculate the total energy absorbed. For this investigation, an impact energy of 48 kJ was imparted into the system.

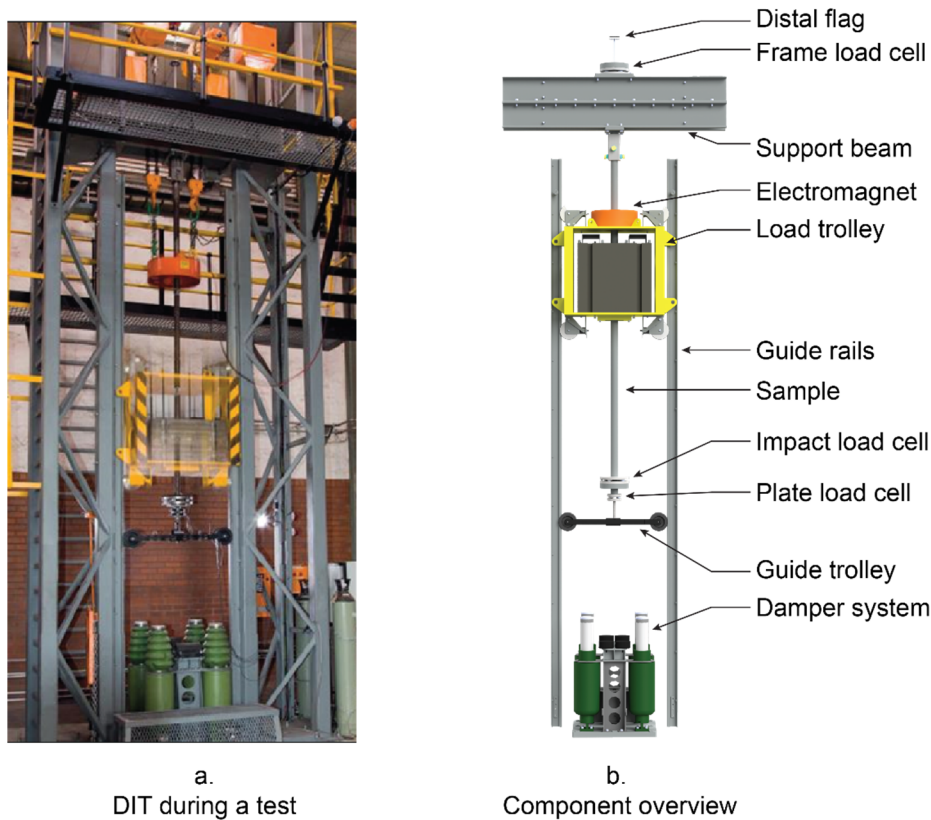


Figure 8 Illustration of the Epiroc DIT (Abreu & Knox 2022)

Table 1 Epiroc dynamic impact tester specifications (Abreu & Knox 2022)

Specification	Value
Max. impulse	65 kJ
Max. impact velocity	6.42 m/s
Max. drop mass	3,171 kg
Min. drop mass	551 kg
Max. drop height	2.1 m
Max. sample length	3.5 m
Height of structure	8.2 m

4 Evaluation of the mobilised length and dynamic performance

A total of 15 samples were prepared and tested for this investigation. Of the 15 samples, the results of two samples were discarded during testing, both resulting from instrumentation failure (cable damage). Consequently, the validity of this data was comprised. The results of the remaining 13 samples are summarised in Table 2. The distal displacements (δ_{distal}) recorded, measured as illustrated in Figure 7c, ranged between 3 mm to 13 mm across all the samples. Therefore, the majority of the plate displacement (δ_{plate}) recorded, measured as illustrated in Figure 7c, can be attributed to the plastic deformation of the mobilised length of steel. This is visually demonstrated in Figure 9.

The average impact load (AIL) was calculated using the method described by Li et al. (2021); the plastic energy absorbed was divided by the plate displacement. The kJ/m value and strain were determined relative to the mobilised length of steel and not the total length of the rockbolt tested.

Figure 10 depicts the load–deformation response for all the samples. The profile of the load response for all three sample sets is consistent, with the displacement at rupture varying, with greater displacements recorded for greater mobilised lengths.

Table 2 Result summary

Sample reference	Mobilised length (mm)	Plate displacement (mm)	Absorbed energy (kJ)	Distal displacement (mm)	Average impact load (kN)	Energy absorption rate (kJ/m)	Strain (%)
P1R-2018-S01	800	145	33	13	228	41	16
P1R-2018-S02	800	132	30	7	230	38	17
P1R-2018-S03	800	122	28	9	224	34	14
P1R-2018-S04	800	124	28	4	223	35	15
P1R-2021-S01	1,100	177	38	3	216	35	16
P1R-2021-S02	1,100	165	36	9	218	33	14
P1R-2021-S03	1,100	166	34	10	207	31	14
P1R-2021-S04	1,100	184	40	9	217	36	16
P1R-2021-S05	1,100	180	38	9	209	34	16
P1R-2024-S01	1,400	207	44	5	211	31	14
P1R-2024-S02	1,400	198	43	7	215	30	14
P1R-2024-S03	1,400	205	44	4	217	32	14
P1R-2024-S04	1,400	216	48	9	221	34	15

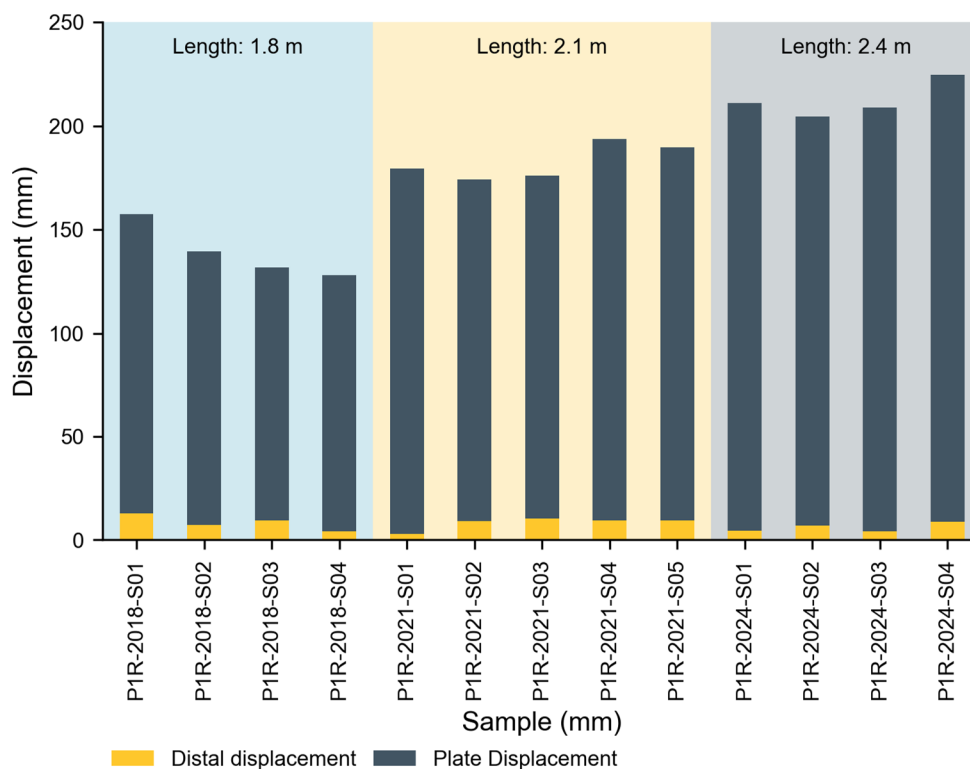


Figure 9 Plate and distal displacement of each sample

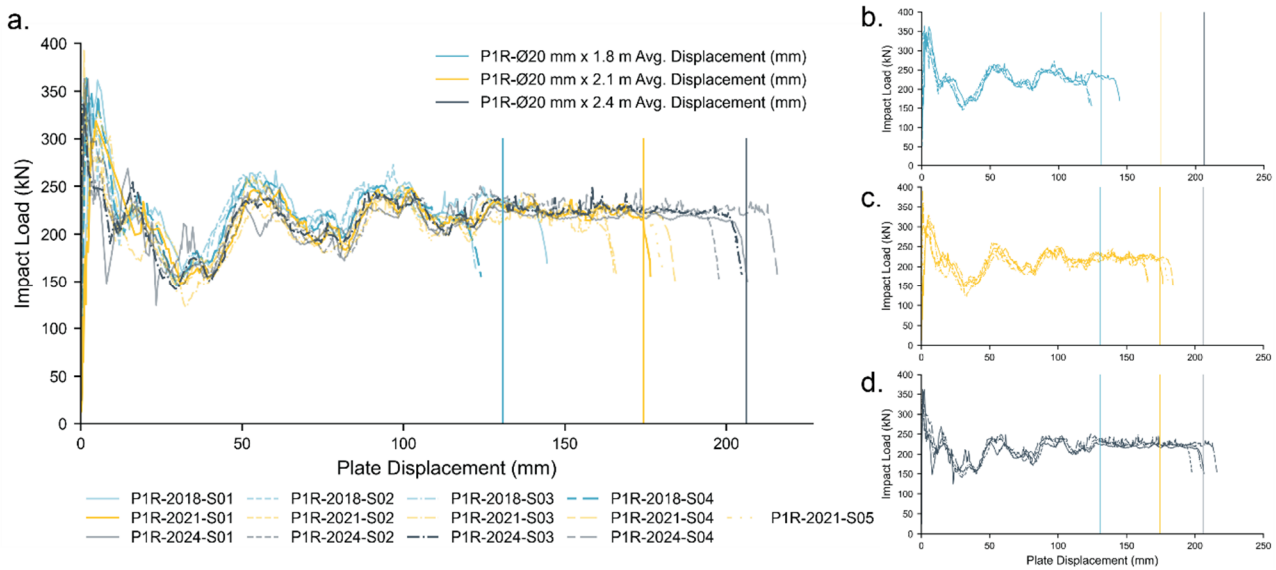


Figure 10 Impact load–displacement plots for the tests. (a) All results; (b) Ø20 × 800 mm mobilised length result; (c) Ø20 × 1,100 mm mobilised length result; (d) Ø20 × 1,400 mm mobilised length result

A summary of the results per sample batch is illustrated in Table 3. The increase in the displacement to rupture and energy absorbed is consistent with the general understanding of the performance of rockbolts. However, the reduction in the energy absorbed per metre of material loaded, and the reduction in strain, highlights the requirement of testing the specific product. While a reduction in the AIL is observed, there was no correlation between the length of the mobilised length and the AIL calculated.

Table 3 Batch summary

Batch reference	Mobilised length (mm)	Plate displacement (mm)	Absorbed energy (kJ)	Average impact load (kN)	Distal displacement (mm)	Energy absorption rate (kJ/m)	Strain (%)
P1R-2018	800	131	30	226	8	37	16
P1R-2021	1,100	174	37	213	8	34	15
P1R-2024	1,400	206	45	216	6	32	14

5 Discussion

An increase in the magnitude of the absolute energy absorbed and plate displacement was recorded for longer rockbolt lengths, which was to be anticipated considering the increase in mobilised length. The distal displacement ranged between 1.7 and 9.0% of the mobilised length of the respective samples, demonstrating good quality and consistency of the resin mixture using the paddle set configuration of the PAR1 Resin Bolt. Consequently, the displacement recorded at the proximal end of the rockbolt (the plate displacement) can be mainly attributed to the deformation of the steel. There is no correlation between the distal displacement and mobilised length. A further demonstration of the consistency of the response of the rockbolt is illustrated through the impact load–displacement response of each sample, plotted in Figure 10.

Considering the known strain behaviour of the steel summarised in Section 2, the slight reduction in the average strain from an 800 mm mobilised length to 1,400 mm was anticipated. Consequently, the reduction in energy absorbed per metre of debonded length is logical; the total energy absorbed is calculated as the product of the impact load and the displacement to rupture. This highlights the importance of understanding 1) the length of the mobilised steel when reviewing a test result and 2) that the performance of rockbolts should not be extrapolated.

If it were assumed that the data from the 1.8 m Ø20 mm PAR1 Resin Bolt was to be used to estimate the performance of a 2.4 m length equivalent, the estimated displacement capacity would be 210 mm and the energy absorption capacity would be 52 kJ. Both values exceed the average performance recorded during this testing program for rockbolts produced from the same steel.

Therefore, these results demonstrate that performance data should not be extrapolated from shorter rockbolts to determine the displacement and energy absorption capacity of longer rockbolts.

The rockbolts tested for this investigation were all manufactured from the same batch of steel. Future work should include an investigation into the effect of variation of the mechanical properties of the steel bar, resulting from variations between steel casts, on the energy absorption capacity of the rockbolt.

6 Conclusion

The objective of the testing program was to demonstrate the effect of the debonded length of steel which in turn affects the length of steel mobilised during loading. Padded energy-absorbing rockbolts absorb energy through the plastic deformation of steel. Consequently, the capacity of a rockbolt is directly correlated to the performance of the mechanical and geometric properties of the steel from which it is produced.

Due to the inaccessibility, cost of operation and design of impact test laboratories, results are often extrapolated from shorter samples. For this investigation, three batches of PAR1 Resin Bolts of varying lengths were prepared and tested using the Epiroc DIT. The lengths were varied to vary the debonded length. The sourcing and preparation of the samples were controlled. Hence, the parameters of the investigation were controlled.

An increase in energy and displacement capacity was observed with an increase in length, consistent with the assumption employed when extrapolating data. However, the reduction of normalised parameters (energy absorption rate and strain) illustrated that the practice of extrapolating to longer mobilised lengths using data generated from shorter samples can result in an overestimation of the energy absorption capacity of a rockbolt.

Acknowledgement

The contribution of Lwazi Pambuka and his team in operating the testing facility is gratefully acknowledged.

References

- Abreu, R & Knox, G 2022, 'The influence of drilling on the performance of a yielding self-drilling rockbolt', in Y Potvin (ed.), *Caving 2022: Fifth International Conference on Block and Sublevel Caving*, Australian Centre for Geomechanics, Perth, pp. 165–176, https://doi.org/10.36487/ACG_repo/2205_09
- ASTM International 2008, *Standard Test Method for Laboratory Determination of Rock Anchor Capabilities by Pull and Drop Tests (ASTM D7401 [withdrawn])*, ASTM International, West Conshohocken.
- ASTM International 2022, *Standard Test Methods and Definitions for Mechanical Testing of Steel Products (ASTM A370-22)*, ASTM International, West Conshohocken.
- Bosman, K, Cawood, M & Berghorst, A 2018, 'Relationship between energy per impulse and dynamic capacity of a rockbolt', in *Rock Dynamics and Applications*, 3rd edn, CRC Press, Boca Raton.
- Epiroc 2023, *PAR1 Resin Bolt*, viewed 2 February 2023, Epiroc, Stockholm, <https://www.epiroc.com/en-ba/products/rock-drilling-tools/ground-support/energy-absorbing-rockbolts/par1-resin-bolt>
- Hadjigeorgiou, J & Potvin, Y 2011, 'A critical assessment of dynamic rock reinforcement and support testing facilities', *Rock Mechanics and Rock Engineering*, vol. 44, pp. 565–578.
- International Organization for Standardization 2019, *Metallic Materials—Tensile Testing—Part 1: Method of Test at Room Temperature, ISO 6892-1:2019*, International Organization for Standardization, Geneva.
- Kaiser, PK & Moss, A 2022, 'Deformation-based support design for highly stressed ground with a focus on rockburst damage mitigation', *Journal of Rock Mechanics and Geotechnical Engineering*, vol. 14, no. 1, pp. 50–66.
- Knox, G, Berghorst, A & Crompton, B 2018a, 'The relationship between the magnitude of impact velocity per impulse and cumulative absorbed energy capacity of a rock bolt', *Proceedings of the 4th Australian Ground Control in Mining Conference*, Australasian Institute of Mining and Metallurgy, Melbourne, pp. 160–169.
- Knox, G & Berghorst, A 2018a, 'Increased agility for the research and development of dynamic roof support products', in *Rock Dynamics Experiments, Theories and Applications*, CRC Press, Boca Raton, pp. 373–384.

- Knox, G & Berghorst, A 2018b, 'Proposed new multiple split tube testing method for dynamic ground support used in highly fractured ground', *CIM 2018 Convention*, Canadian Institute of Mining, Metallurgy and Petroleum, Westmount.
- Knox, G, Berghorst, A & de Bruin, P 2018, 'An empirical comparison between new and existing laboratory-based dynamic sample configurations', in Y Potvin & J Jakubec (eds), *Caving 2018: Proceedings of the Fourth International Symposium on Block and Sublevel Caving*, Australian Centre for Geomechanics, Perth, pp. 747–758, https://doi.org/10.36487/ACG_rep/1815_58_Knox
- Knox, G & Hadjigeorgiou, J 2022, 'Influence of testing configuration on the performance of paddled energy-absorbing rockbolts under impact loading', *Rock Mechanics and Rock Engineering*, vol. 55, pp. 5705–5721.
- Li, CC 2010, 'A new energy-absorbing bolt for rock support in high stress rock masses', *International Journal of Rock Mechanics and Mining Sciences*, vol. 47, 3rd edn, pp. 396–404.
- Li, CC & Doucet, C 2012, 'Performance of D-bolts under dynamic loading conditions', *Rock Mechanics and Rock Engineering*, vol. 45, 2nd edn, pp. 193–204.
- Li, CC, Hadjigeorgiou, J, Mikula, P, Knox, G, Darlington, B, Royer, R, ... Hosp, M 2021, 'Performance of identical rockbolts tested on four dynamic testing rigs employing the direct impact method', *Journal of Rock Mechanics and Geotechnical Engineering*, vol. 13, 4th edn, CSRME, pp. 745–754.
- Tec Science 2018, *Tec Science*, viewed 18 February 2018, <https://www.tec-science.com/material-science/material-testing/tensile-test/>